This article was downloaded by: [207.114.134.62]
On: 21 July 2014, At: 08:08
Publisher: Taylor & Francis
Informa Ltd Registered in England and Wales Registered Number: 1072954 Registered office: Mortimer House, 37-41 Mortimer Street, London W1T 3JH, UK

Journal of the Air & Waste Management Association
Publication details, including instructions for authors and subscription information:
http://www.tandfonline.com/loi/uawm20

The potential near-source ozone impacts of upstream oil and gas industry emissions

Eduardo P. Olaguer [a]

[a] Houston Advanced Research Center , The Woodlands , Texas , USA

Accepted author version posted online: 29 May 2012.Published online: 18 Jul 2012.

To cite this article: Eduardo P. Olaguer (2012) The potential near-source ozone impacts of upstream oil and gas industry emissions, Journal of the Air & Waste Management Association, 62:8, 966-977, DOI: 10.1080/10962247.2012.688923

To link to this article: http://dx.doi.org/10.1080/10962247.2012.688923

PLEASE SCROLL DOWN FOR ARTICLE

Taylor & Francis makes every effort to ensure the accuracy of all the information (the “Content”) contained in the publications on our platform. However, Taylor & Francis, our agents, and our licensors make no representations or warranties whatsoever as to the accuracy, completeness, or suitability for any purpose of the Content. Any opinions and views expressed in this publication are the opinions and views of the authors, and are not the views of or endorsed by Taylor & Francis. The accuracy of the Content should not be relied upon and should be independently verified with primary sources of information. Taylor and Francis shall not be liable for any losses, actions, claims, proceedings, demands, costs, expenses, damages, and other liabilities whatsoever or howsoever caused arising directly or indirectly in connection with, in relation to or arising out of the use of the Content.

This article may be used for research, teaching, and private study purposes. Any substantial or systematic reproduction, redistribution, reselling, loan, sub-licensing, systematic supply, or distribution in any form to anyone is expressly forbidden. Terms & Conditions of access and use can be found at http://www.tandfonline.com/page/terms-and-conditions

TECHNICAL PAPER

The potential near-source ozone impacts of upstream oil and gas industry emissions

Eduardo P. Olaguer*

Houston Advanced Research Center, The Woodlands, Texas, USA

**Please address correspondence to: Eduardo P. Olaguer, Houston Advanced Research Center, 4800 Research Forest Dr., The Woodlands, TX 77381, USA; e-mail: eolaguer@harc.edu*

Increased drilling in urban areas overlying shale formations and its potential impact on human health through decreased air quality make it important to estimate the contribution of oil and gas activities to photochemical smog. Flares and compressor engines used in natural gas operations, for example, are large sources not only of NO_x but also of formaldehyde, a hazardous air pollutant and powerful ozone precursor. We used a neighborhood scale (200 m horizontal resolution) three-dimensional (3D) air dispersion model with an appropriate chemical mechanism to simulate ozone formation in the vicinity of a hypothetical natural gas processing facility, based on accepted estimates of both regular and nonroutine emissions. The model predicts that, under average midday conditions in June, regular emissions mostly associated with compressor engines may increase ambient ozone in the Barnett Shale by more than 3 ppb beginning at about 2 km downwind of the facility, assuming there are no other major sources of ozone precursors. Flare volumes of 100,000 cubic meters per hour of natural gas over a period of 2 hr can also add over 3 ppb to peak 1-hr ozone somewhat further (>8 km) downwind, once dilution overcomes ozone titration and inhibition by large flare emissions of NO_x. The additional peak ozone from the hypothetical flare can briefly exceed 10 ppb about 16 km downwind. The enhancements of ambient ozone predicted by the model are significant, given that ozone control strategy widths are of the order of a few parts per billion. Degrading the horizontal resolution of the model to 1 km spuriously enhances the simulated ozone increases by reducing the effectiveness of ozone inhibition and titration due to artificial plume dilution.

Implications: Major metropolitan areas in or near shale formations will be hard pressed to demonstrate future attainment of the federal ozone standard, unless significant controls are placed on emissions from increased oil and gas exploration and production. The results presented here show the importance of improving the temporal and spatial resolution of both emission inventories and air quality models used in ozone attainment demonstrations for areas with significant oil and gas activities.

Supplemental Materials: Supplemental materials are available for this article. Go to the publisher's online edition of the *Journal of the Air & Waste Management Association* for further technical details on the HARC model chemical mechanism and its performance evaluation.

Introduction

The Barnett Shale as an indicator of potential air quality problems

The air quality impacts of oil and gas exploration and production (E&P) are the subject of increasing scrutiny. In Texas, considerable attention has been focused on the Barnett Shale because of public concern over industry emissions of hazardous air pollutants (HAPs), such as benzene and formaldehyde. Ambient whole air sampling by Wolf Eagle Environmental (2009) in Dish, Texas, indicated levels of a number of HAPs in excess of both short-term and long-term effects screening levels (ESLs). These high concentrations appeared to implicate oil and gas activities in the vicinity, particularly of compressor stations used to feed natural gas pipelines.

Oil and gas activities in the Barnett Shale not only may expose the public to toxic air pollutants, but also may contribute to smog in the Dallas–Fort Worth (DFW) ozone nonattainment area, which has yet to attain the former U.S. 8-hr ozone standard of 85 ppb, let alone the current 75 ppb standard. Regional background ozone in DFW can be as high as 55–60 ppb, leaving little room for local emissions of ozone precursors (Kemball-Cook et al., 2009). This poses a severe challenge to oil and gas producers in the DFW area, as urban drilling and the associated growth in industry emissions may be sufficient to keep the area in nonattainment.

The current state of the art in estimating oil and gas field emissions primarily involves handbook estimates, mainly those provided by the U.S. Environmental Protection Agency (EPA) AP-42 methodology. A survey of relevant estimation methods is given by Bar-Ilan et al. (2008). Using these methods, Armendariz (2009) estimated peak summer emissions of ozone precursors in

Journal of the Air & Waste Management Association, 62(8):966–977, 2012. Copyright © 2012 A&WMA. ISSN: 1096-2247 print
DOI: 10.1080/10962247.2012.688923

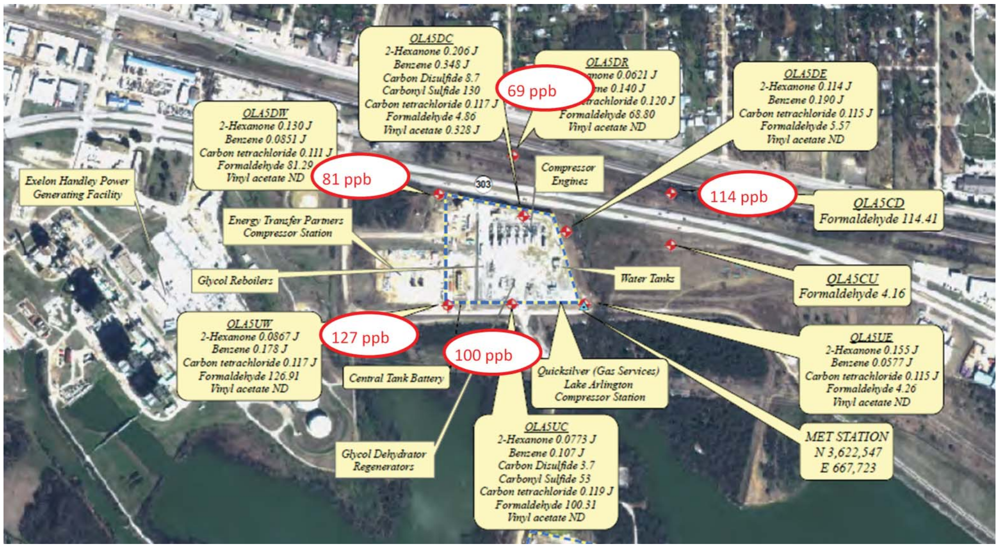
OLA5DC
2-Hexanone 0.206 J
Benzene 0.348 J
Carbon Disulfide 8.7
Carbonyl Sulfide 130
Carbon tetrachloride 0.117 J
Formaldehyde 4.86
Vinyl acetate 0.328 J
69 ppb
OLA5DR
none 0.0621 J
ne 0.140 J
trachloride 0.120 J
Formaldehyde 68.80
Vinyl acetate ND
OLA5DE
2-Hexanone 0.114 J
Benzene 0.190 J
Carbon tetrachloride 0.115 J
Formaldehyde 5.57
Vinyl acetate ND
OLA5DW
2-Hexanone 0.130 J
Benzene 0.0851 J
Carbon tetrachloride 0.111 J
Formaldehyde 81.29
Vinyl acetate ND
81 ppb
Exelon Handley Power Generating Facility
303
Compressor Engines
114 ppb
OLA5CD
Formaldehyde 114.41
Energy Transfer Partners Compressor Station
Glycol Reboilers
Water Tanks
OLA5CU
Formaldehyde 4.16
OLA5UW
2-Hexanone 0.0867 J
Benzene 0.178 J
Carbon tetrachloride 0.117 J
Formaldehyde 126.91
Vinyl acetate ND
127 ppb
100 ppb
Central Tank Battery
Quicksilver (Gas Services) Lake Arlington Compressor Station
OLA5UE
2-Hexanone 0.155 J
Benzene 0.0577 J
Carbon tetrachloride 0.115 J
Formaldehyde 4.26
Vinyl acetate ND
Glycol Dehydrator Regenerators
OLA5UC
2-Hexanone 0.0773 J
Benzene 0.107 J
Carbon Disulfide 3.7
Carbonyl Sulfide 53
Carbon tetrachloride 0.119 J
Formaldehyde 100.31
Vinyl acetate ND
MET STATION
N 3,622,547
E 667,723

Figure 1. 1-hr measurements of HCHO (indicated in red) and other air toxics at the Quicksilver Lake Arlington site in Fort Worth on the morning of July 11, 2010 (adapted from BSEEC, 2010).

2009 from all oil and gas sources in the Barnett Shale to be 307 tons per day (tpd). By comparison, he estimated on-road mobile emissions from the five counties in the DFW ozone nonattainment area with significant oil and gas production in 2009 to be 121 tpd.

Since 2009, there have been a number of studies utilizing standard U.S. EPA monitoring methods to increase local knowledge of air emissions and impacts due to Barnett Shale E&P activities. For example, the Texas Commission on Environmental Quality (TCEQ) has put up several new automated gas chromatograph (auto-GC) stations, and has also conducted mobile auto-GC measurements in various areas. The Barnett Shale Energy Education Council (BSEEC) hired Titan Engineering to conduct both 1-hr and 24-hr Summa canister and DNPH cartridge sampling at 10 natural gas sites (BSEEC, 2010). More recently, the City of Fort Worth hired Eastern Research Group, Inc. (ERG), to conduct ambient air quality monitoring using Summa canisters and DNPH cartridges at seven fixed sites, together with point source emission sampling using toxic vapor analyzers (TVAs) at a large number of oil and gas facilities (ERG, 2011).

Figure 1 shows 1-hr ambient monitoring data collected at a pipeline compressor station in Lake Arlington, Fort Worth, during the BSEEC study. Note the very large short-term concentrations of formaldehyde (HCHO) approaching or exceeding 100 ppb around the site. Such large concentrations may be cause for concern, not only because of short-term health impacts such as nosebleeds, vomiting, and skin irritation, but also because of formaldehyde's capacity to release radicals and thus contribute to rapid ozone formation (Olaguer et al., 2009). To date, no credible explanation has ever been given for these observations. Short-term, near-road sampling of ambient air using DNPH cartridges has never detected more than about 17 ppb of HCHO in the United States (HEI, 2007), thereby ruling out mobile sources as a likely cause. The brisk southerly wind prevailing on the morning of July 11, 2010, is not consistent with transport of pollution from the natural gas-fired power plant immediately to the west of the compressor station. On the other hand, it does not rule out air counterflow due to on-site structures, possibly explaining elevated HCHO levels at the upwind edge of the facility. The short-term sampling conducted by Titan Engineering was limited to a single hour, so it is difficult to determine if the high ambient HCHO was due to an emission event at the compressor station (e.g., due to engine maintenance).

Based on dispersion modeling conducted by ERG as part of the Fort Worth Air Quality Study, the HAPs emitted by oil and gas sources identified as posing the greatest human health risk were acrolein, benzene, and formaldehyde. The maximum 1-hr average HCHO concentration predicted outside the fence line based on regular (i.e., routine) emissions from a hypothetical worst-case compressor station was 34.7 ppb. No dispersion modeling was conducted for a natural gas processing facility, although ERG's emission estimates indicate that such as facility may emit twice as much formaldehyde as a compressor station.

To perform the health risk assessment, ERG relied on standard emission factors to derive estimates of regular emissions from surveyed engines, and ignored nonroutine emissions from flares. This was because the conventional monitoring technology used by ERG could not quantify combustion emissions of formaldehyde and other volatile organic compounds (VOCs) from either compressor engines or flares. Table 1 summarizes the largest point sources found by ERG based on a combination of point source monitoring (where applicable) and estimates derived from standard emission factors and equipment surveys. It appears that the point source facility types of greatest concern are natural gas processing facilities and pipeline compressor stations, mostly because of regular emissions from compressor engines, which ERG conservatively assumed were operating uncontrolled 24 hr/day, seven days per week.

ERG did not document any process upsets, startups, shutdowns, or maintenance that could have led to emission events at the targeted oil and gas sites. Publicly available data on such activities and their associated releases to air are sparse for the upstream oil and gas industry in Texas, unlike for the downstream petrochemical industry in the Houston region, where

Table 1. Largest point sources identified in the Fort Worth Air Quality Study (ERG, 2011)

			VOCs (tons/yr)				HAPs (tons/yr)	
Site ID Site Type	NO_x (tons/yr)	CO (tons/yr)	Total	Engine	Tank	Fugitive	Total	HCHO
PS-159 PF*	87.74	1038.90	79.93	79.58	<0.01	0.34	47.32	31.93
PS-118 CS*	51.42	269.95	42.69	42.59	<0.01	0.11	25.31	17.08
PS-119 CS*	45.77	240.30	37.80	37.79	<0.01	0.01	22.46	15.16
PS-127 CS*	24.33	545.08	23.70	23.56	0.11	0.04	14.02	9.45
238 WP*	15.71	219.33	14.24	14.12	0.11	<0.01	8.42	5.67

Note. PF, processing facility, CS, compressor station, WP, well pad.

facilities are required by the TCEQ to report emissions exceeding 1200 lb/hr of highly reactive VOCs (HRVOCs, defined as the olefins: ethene, propene, 1,3-butadiene, and butenes). A significant acknowledged source of HRVOCs is flaring of waste gas.

Table 2 presents data on upstream oil and gas flares collected by the Alberta Energy Utilities Board as summarized by Argo (2011). Note the relatively frequent occurrence of flare volumes between 1000 and 10,000 × 10^3 m^3/day (i.e., as much as several hundred cubic meters per second) at gas plants and other upstream facilities. As of 2004, there were 166 natural gas processing plants in Texas with a total capacity of a little less than half a billion cubic meters per day (EIA, 2006). Such huge volumes demand a rigorous investigation as to their likely air quality impacts.

Questions posed

Our objective in this study was to answer the following questions:

(1) How important are nonroutine flares and possibly other emission events compared to regular emissions from compressor engines used in oil and gas facilities with respect to their ozone formation potential?
(2) How far from the source are significant ozone impacts likely to be seen?
(3) What are the most important ozone precursors to control in order to mitigate the ozone impacts of oil and gas activities?

To answer these questions, we conducted a schematic modeling exercise that was not intended to implicate any actual operational facility, but only to provide reasonable quantitative bounds. For convenience, we assumed that a hypothetical natural gas processing facility was located sufficiently far away from major roadways or other intense anthropogenic sources of ozone precursors, and used model input data largely derived from the Fort Worth Air Quality Study, except for flare emission data, which were not collected by ERG.

Table 2. Flare volumes (1000 m^3/day) at Alberta sour gas sites in 1996 after Argo (2011)

Gas plants			Gas gathering		
Volume range		Number of sites	Volume range		Number of sites
0.1	1	3	1	10	2
1	10	21	10	100	23
10	100	61	100	1000	31
100	1000	124	1000	10000	51
1000	10000	53	10000	100000	15
10000	50000	3			
Total sour gas plants		265	Total gathering systems		122
Batteries			Townships		
0.1	1	152	0.1	1	29
1	10	736	1	10	87
10	100	1847	10	100	233
100	1000	2113	100	1000	555
1000	10000	388	1000	10000	480
10000	50000	8	10000	50000	26
Total batteries		5244	Total townships		1410

Methodology

The HARC neighborhood air quality model

The Houston Advanced Research Center (HARC) recently developed a neighborhood scale (~100 m × 100 m horizontal resolution) Eulerian air quality model coded in MATLAB, and used it to demonstrate an adjoint modeling technique for performing computer-aided tomography (CAT) based on remote-sensing measurements (Olaguer, 2011). We have added online photochemistry to the HARC model in order to investigate the near source ozone impacts of industrial emissions of reactive species, such as olefins and formaldehyde.

Rapid ozone chemistry associated with large point-source emissions of reactive species may not be well simulated by conventional air quality models due to their relatively low spatial resolution. For example, the air quality model used to demonstrate ozone attainment in the most recent U.S. EPA-approved Texas State Implementation Plan (SIP) for the DFW area has a horizontal resolution of 4 km × 4 km (TCEQ, 2007). Plume-in-grid treatments of sub-grid-scale dispersion are primarily intended to address the net effects of small plumes on grid-scale concentrations, and not to explicitly simulate fine concentration gradients. While other modeling approaches exist, such as Lagrangian reactive plume, large eddy simulation, and adaptive grid techniques, a major barrier to very-high-resolution simulations of reactive species is the computational cost of current chemical mechanisms intended to simulate urban to regional and even continental scales.

The HARC air quality model combines accepted treatments of pollutant transport with a highly efficient chemical mechanism designed explicitly for neighbourhood-scale applications. The model architecture is summarized only briefly here, with further details provided in the Supporting Information. The most important features of the model transport are listed in Table 3. Note that the HARC advection and diffusion solvers are identical to those used in the U.S. EPA Community Multiscale Air Quality (CMAQ) model (Byun and Ching, 1999).

The HARC chemical mechanism has 47 reactions, with standard urban NO_x-O_3 photochemistry, and detailed schemes for the radical precursors, formaldehyde and nitrous acid, as well as the olefins considered HRVOCs by the Texas SIP (see earlier discussion). Abbreviated schemes were included for isoprene (based on CB05; see Yarwood et al., 2005) and the aromatics, toluene and xylene (based on CB05-TU; see Whitten et al., 2010), ignoring longer lived intermediates such as methacrolein, methyl vinyl ketone, and cresol. Less reactive organics, including alkanes and oxygenates such as acetaldehyde, were lumped together and assigned a total OH reactivity, denoted by r_{BVOC}. Photolysis rates were parameterized according to Saunders et al., (2003). Nonphotolytic reaction rates were obtained from NASA Jet Propulsion Laboratory (2006, 2010), CB05, SAPRC07 (Carter, 2010), or the Master Chemical Mechanism (MCM; see Saunders et al., 2003). An evaluation of the HARC mechanism based on data from the 2006 TRAMP experiment (Chen et al., 2010) is provided in the Supporting Information, and shows that the HARC mechanism performs as well as established mechanisms in simulating the urban radical budget.

The HARC mechanism is accompanied by a simplified chemical solver based on the Euler backward iterative (EBI) scheme of Hertel et al. (1993) for the chemical group consisting of NO, NO_2 and O_3, and the assumption of chemical equilibrium for HO_x species. (Note: The CMAQ model uses the EBI scheme as one of several alternative chemical solvers.) A noniterative backward Euler scheme was used for tracers other than NO_x or O_3. Because of its efficiency, computational time steps of the order of tens of seconds may be employed with the HARC scheme. For this study, we used a 20-sec time step and a horizontal resolution of 200 m. This combination avoids Cauchy-Friedrichs-Lewy instability for wind speeds of ~5 m/sec and ensures that the assumption of HO_x equilibrium is valid at NO concentrations of ~0.5 ppb.

The model scenario

We now proceed to investigate the ozone impacts of a hypothetical natural gas processing facility in the Barnett Shale, located at latitude 33 °N (parameterized photolysis rates are independent of longitude) and 2.5 grid diagonals away from the southwest corner of the model domain, which is either

Table 3. HARC model transport features

Model geometry and physics	Numerical treatment
Domain	4 km × 4 km or 12 km × 12 km horizontal domain; 1 km vertical domain.
Spatial resolution	200 m uniform horizontal resolution; 50 m uniform vertical resolution.
Temporal evolution	Time step: 20 sec Time splitting order:Emission/deposition/chemistry, vertical diffusion, E–W advection, E–W diffusion, N–S advection, N–S diffusion.
Horizontal advection	Piecewise parabolic method (Colella and Woodward, 1984); positive definite zero-flux outflow at boundaries; uniform horizontal wind.
Horizontal diffusion	Explicit scheme; zero gradient (Neumann) boundary conditions; uniform horizontal eddy diffusion coefficient.
Vertical diffusion	Semi-implicit (Crank–Nicholson) scheme; zero-flux boundary condition; vertical diffusion coefficient specified from similarity theory.

Table 4. Transported species parameters

Species	Inflow boundary condition (ppb)	Deposition velocity (cm/sec)	Compressor engine emissions (g/sec)	Flare emission rate (g/sec)
Nitric oxide (NO)	0.41	3×10^{-9}	2.52	32.67
Nitrogen dioxide (NO_2)	0.54	0.35	0.28	3.63
Ozone (O_3)	46.4	0.6		
Nitrous acid (HONO)	0.2	0.3		
Formaldehyde (HCHO)	0.931	0.4	1.01	10.6
Carbon monoxide (CO)	200		32.9	199
Ethene (C_2H_4)	1.12			
Propene (C_3H_6)	0.45			43.4
1,3-Butadiene (C_4H_6)	0.057			
1-Butene (BUT1ENE)	0.2			
2-Butene (BUT2ENE)	0.289			
Isobutene (IBUTENE)	0.291			
Isoprene (ISOP)	0.5			
Toluene (TOL)	0.876			
Xylene (XYL)	0.547			

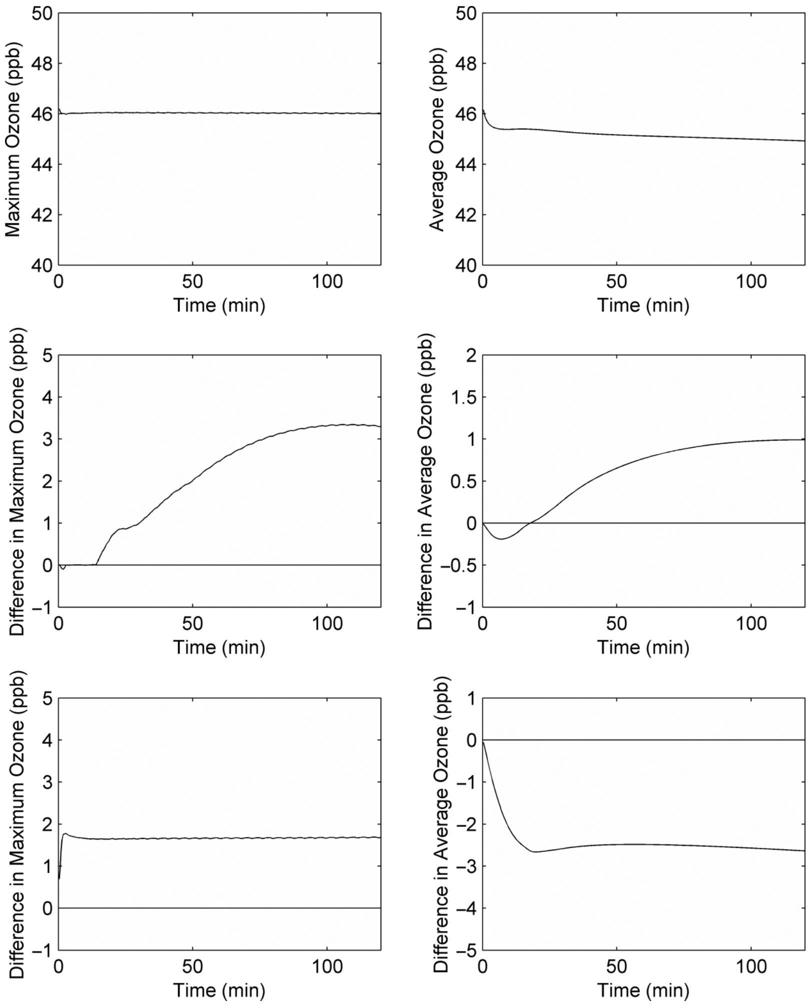

Figure 2. Time series of peak ozone (left) and domain average ozone (right) at the surface for the 4 km × 4 km simulation. Top: Results for control simulation (no facility emissions). Middle: Difference in results between Case 1 (regular emissions) and control simulation. Bottom: Difference in results between Case 2 (flare emission event) and control simulation.

4 km × 4 km or 12 km × 12 km in horizontal extent, and 1 km in vertical extent. No other anthropogenic or biogenic sources were assumed within the model domain.

Meteorology was treated very simply in the model scenario. Vertical wind was ignored. Advection was solely due to a uniform horizontal wind from the southwest. The horizontal diffusion coefficient K_H was set at 50 m^2/sec. The wind speed, surface temperature, and relative humidity were set at 4.8 m/sec, 308.3 K, and 33.5% respectively, corresponding to average conditions at 1 p.m. CST in June 2011 at the Fort Worth NW CAMS 13 monitor. The surface pressure was kept constant at 1 atm. The temperature lapse rate was assumed to be superadiabatic and uniform at 12°C/km. The nonuniform vertical diffusion coefficient K_v associated with the unstable stratification was computed from the analytical formula of McRae et al., (1982), with an inversion height of 1 km, a Monin–Obukhov length of -100 m, and a friction velocity equal to one-third of the horizontal wind speed. The turbulence parameterization of McRae et al. (1982) is similar to that used in the complex hazardous air release model (CHARM), a local dispersion model for emergency planning (Eltgroth, 2012). Although the HARC model has an adjoint modeling capability that allows one to adjust turbulence parameters to improve agreement with chemical species observations (Olaguer, 2011), we did not employ that option for this study.

Table 4 summarizes the boundary conditions and deposition velocities assigned to each advected species in the model. The inflow boundary conditions for CO, O_3, and NO_x species were derived from observations at 1 p.m. CST averaged for June 2011 at the Fort Worth NW CAMS 13 monitor, while those for VOCs other than organic nitrate (RNO_3) were taken from program average measurements during the Fort Worth Air Quality Study. The maximum observed concentration, however, was used for isoprene, the emissions of which vary with insolation. Inflow boundary conditions for HONO and RNO_3 were based on typical midday measurements from the 2006 TRAMP study. The deposition velocities were set to daytime values used in the box model evaluation of various chemical solvers by Huang and Chang (2001), except for HONO, the adopted value for which was based on Stutz et al. (2002).

Table 4 also specifies the emission rates used in our experiment for two cases: (1) regular emissions quantified by ERG, mostly associated with compressor engines; and (2) a hypothetical flare emission event associated with acid gas injection compressor failure at an inlet sour gas separator. NO_x emissions are assumed to be partitioned between NO and NO_2 at a ratio of 9:1.

The emissions for Case 1 were derived from Table 1, ignoring VOCs other than HCHO, as they are either too dilute or much less reactive compared to HCHO to significantly affect ozone

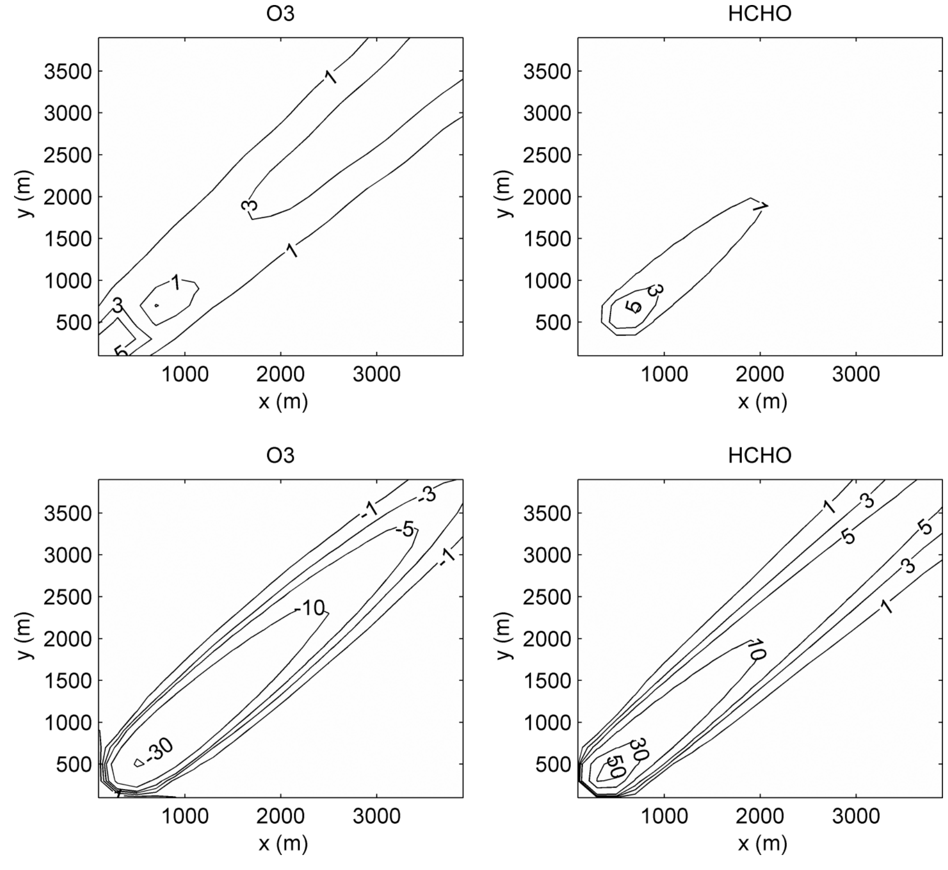

Figure 3. Surface isopleths of O_3 (left) and HCHO (right) mixing ratio (ppb) at the surface at the end of the 4 km × 4 km simulation. Top: Difference in results between Case 1 (regular emissions) and control simulation. Bottom: Difference in results between Case 2 (flare emission event) and control simulation. Unequally spaced contour intervals are used for concentration values equal to $(1, 3, 5) \times 10^n$, where n is an integer.

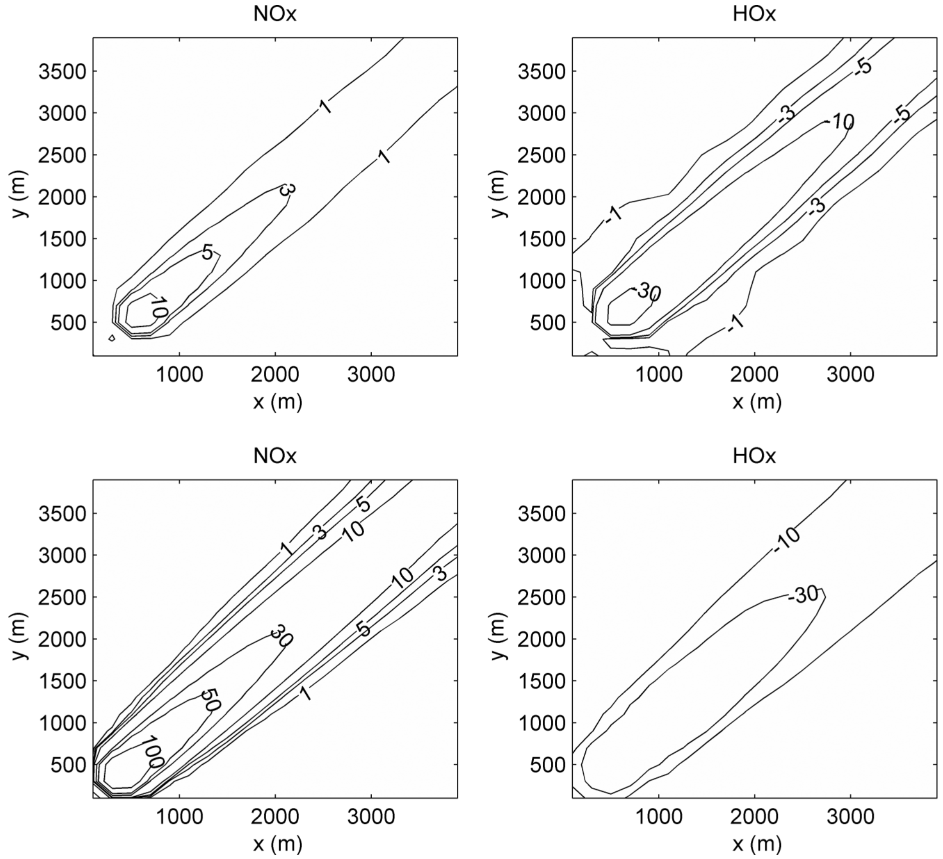

Figure 4. Same as in Figure 3, but for NO_x (left) and HO_x (right). The HO_x mixing ratios are in parts per trillion (ppt).

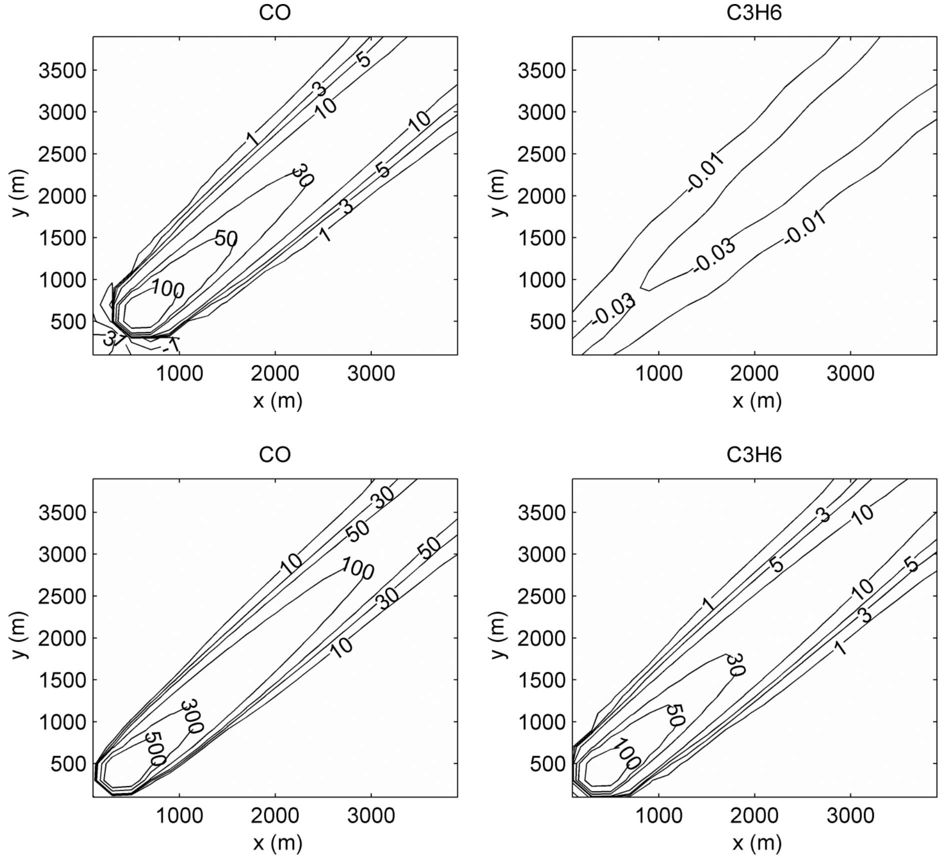

Figure 5. Same as in Figure 3, but for CO (left) and C_3H_6 (right).

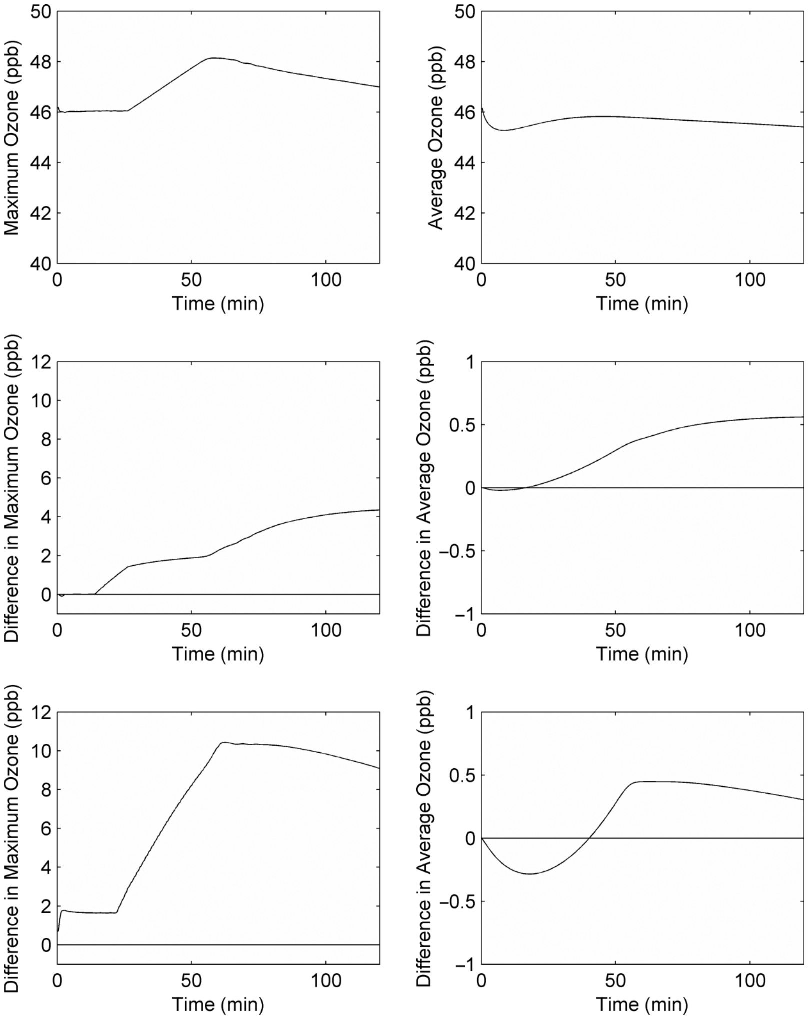

Figure 6. Same as in Figure 2, but for 12 km × 12 km domain.

formation near the source. The emissions for Case 2 were derived from flare emission factors adopted by the Canadian Association of Petroleum Producers (2004, 2006), but with an assumed HCHO-to-CO molar ratio of 5%, consistent with observations of natural gas flares during the 2010 TCEQ Flare Study (Allen and Torres, 2011; Torres et al., 2011). Note that in the flare case, significant emissions of highly reactive propene were included. The flare emissions were assumed to be continuous over 2 hr, and correspond to a flare volume of 100 × 10^3 m^3/hr of natural gas, with a heating value of 1209 BTU/ft^3 or 4.5 × 10^7 J/m^3, as is typical in the Barnett Shale (Bar-Ilan et al., 2008). The effective release height of the flare was assumed to be within the first model layer above the surface (<50 m AGL).

The model simulation started at 1 p.m. CST on Julian day 180 (June 29) and ended two hr later, coinciding with the duration of the hypothetical flare emission event of Case 2. Regular emissions were assumed to be ongoing throughout the simulation in Case 1, but were suppressed in Case 2. The initial concentrations of advected species in the interior of the domain were set equal to the inflow boundary conditions. The total OH reactivity of unresolved organics, that is, r_{BVOC}, was set at 5 sec^{-1} throughout the simulation, based roughly on program average monitoring data collected by ERG during the Fort Worth Air Quality Study.

Results and Discussion

We begin by examining the HARC model results for a simulation over a 4 km × 4 km horizontal domain, corresponding to the size of a typical grid box in the current DFW SIP model. Figure 2 displays the time series of peak ozone and domain average ozone at the surface for the control simulation, in which there are no facility emissions. It also shows the difference in results between Case 1 (regular emissions) and the control simulation, and also between Case 2 (flare emission event) and the control.

Note that the domain average surface ozone mixing ratio in the control case decreases by about 1 ppb due to NO_x titration ($NO + O_3 \rightarrow NO_2 + O_2$) associated with the inflow boundary conditions, while peak ozone at the surface remains roughly constant. Regular emissions from the facility, on the other hand, have a sufficient radical source in HCHO to overcome NO_x titration and inhibition ($NO_2 + OH \rightarrow HNO_3$), so that both

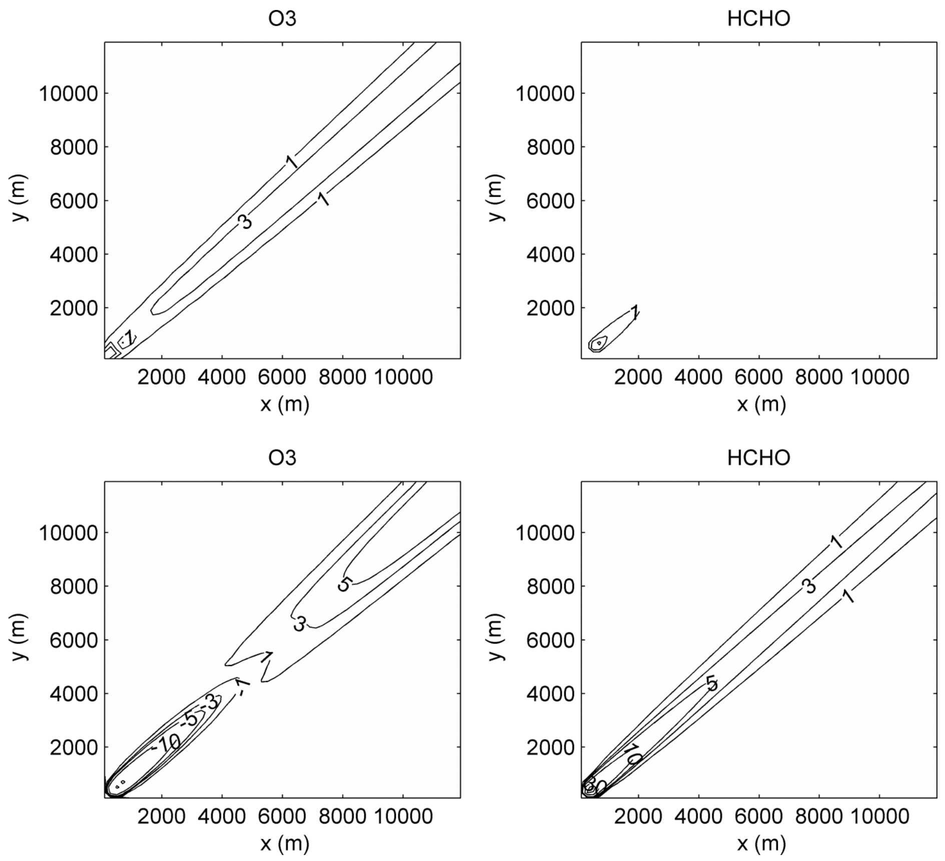

Figure 7. Same as in Figure 3, but for 12 km × 12 km domain.

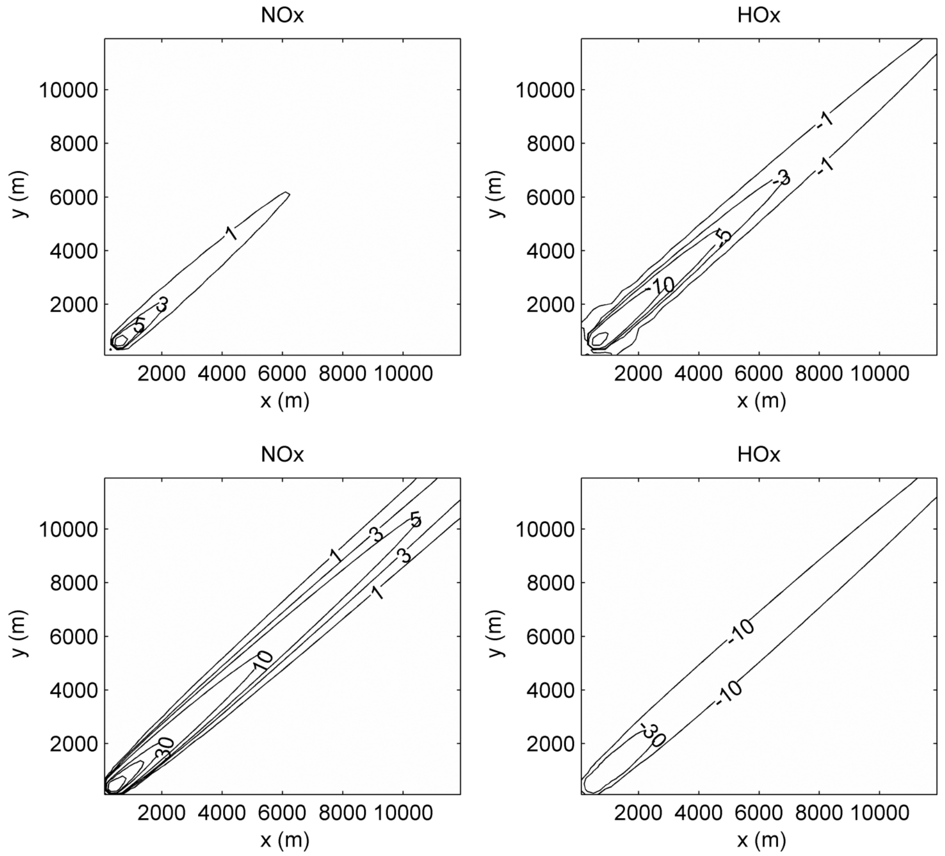

Figure 8. Same as in Figure 4, but for 12 km × 12 km domain.

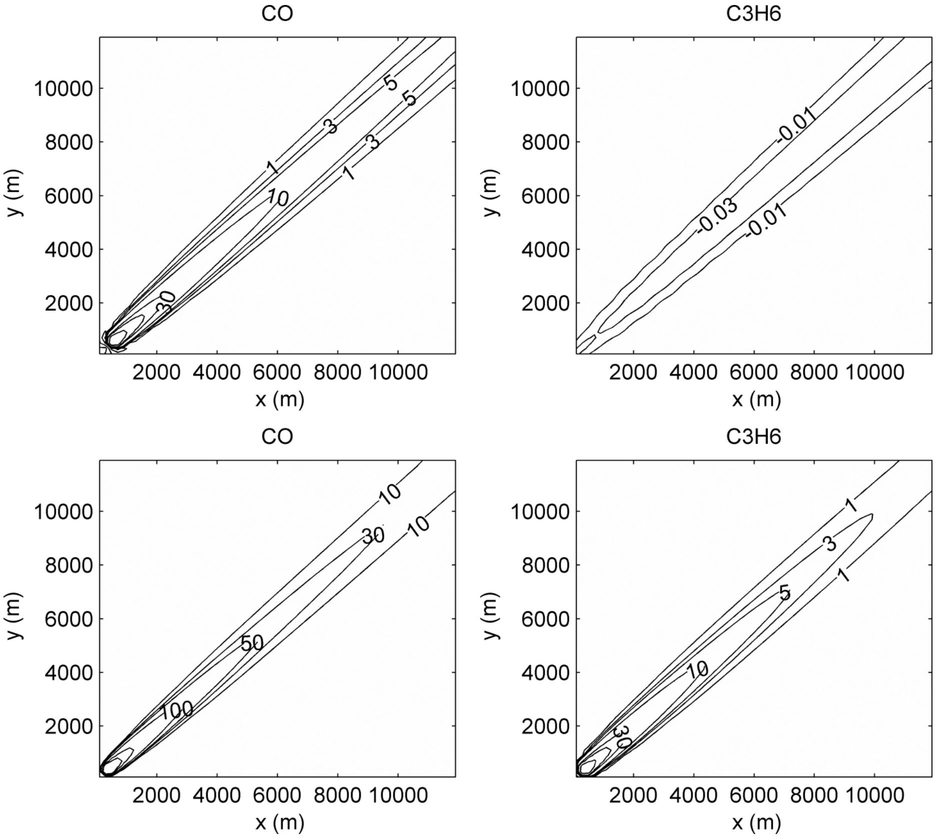

Figure 9. Same as in Figure 5, but for 12 km × 12 km domain.

peak and domain average ozone increase progressively after the first 20 min of the simulation, the former by up to 3 ppb. This results in a significant difference of 2 ppb between peak and domain average ozone in Case 1. The flare emission event, unlike the regular emissions case, depresses domain average ozone by more than 2 ppb due to much larger NO_x emissions, while increasing peak ozone less strongly.

Figures 3–5 show differences in the mixing ratios of several key species between each emission case and the control at the end of the two-hour simulation. An ozone enhancement of 3 ppb or more in the regular emissions plume occurs at distances greater than 2 km downwind of the facility. In the case of the flare emission event, a slight ozone enhancement appears at the upwind corner of the domain, while ozone is depressed downwind, as there is more severe titration of ozone and inhibition of radicals within the flare plume than in the regular emissions case. This is despite concentrations of highly reactive propene exceeding 10 ppb downwind of the flare. Increases in HCHO mixing ratio of 5 ppb or more due to the flare extend all the way to the downwind edge of the domain.

We now consider what happens to the pollution plume from the hypothetical processing facility beyond the confines of the 4 km × 4 km domain. For this we extended the model horizontal domain to 12 km × 12 km and conducted the same 2-hr release experiments for the two emission cases. The results are summarized in Figures 6–9. Note that in the case of the flare emission event, the increase in peak ozone within the expanded domain exceeds 10 ppb about an hour after the flare onset. Ozone enhancements greater than 3 ppb due to the flare appear further downwind (>8 km) of the facility than in the regular emissions case, reflecting the dilution required to overcome NO_x titration and inhibition, and can approach 10 ppb at the edge of the domain about 16 km downwind. The ozone enhancements due to regular emissions still exceed 3 ppb throughout most of the plume. Domain average ozone, on the other hand, is enhanced by no more than ~0.5 ppb in both regular emissions and flare cases.

Finally, we conducted an additional experiment in which we degraded the model horizontal resolution to 1 km on the 12 km × 12 km domain. The differences between the results of the 1-km and 200-m resolution runs are illustrated in Figure 10. Positive differences of up to 6 ppb occur for peak ozone and up to 2 ppb for domain average ozone in the regular emissions case. Even larger differences, up to 22 ppb for peak ozone and up to 3 ppb for domain average ozone, are predicted in the flare case. These differences are due to artificial dilution of both the regular and flare emission plumes, which reduces ozone titration and inhibition by NO_x. This is the opposite of what occurs for very large flares at downstream petrochemical facilities, which often emit more than 1000 lb/hr of olefins and are thus considerably less radical limited. Olaguer (2012) simulated a historical flare in the Houston Ship Channel that emitted more than 1400 lb/hr of ethene. He found a significant decrease in peak ozone downwind of the flare when the model horizontal resolution was degraded from 200 m to 1 km on a 12 km × 12 km horizontal domain.

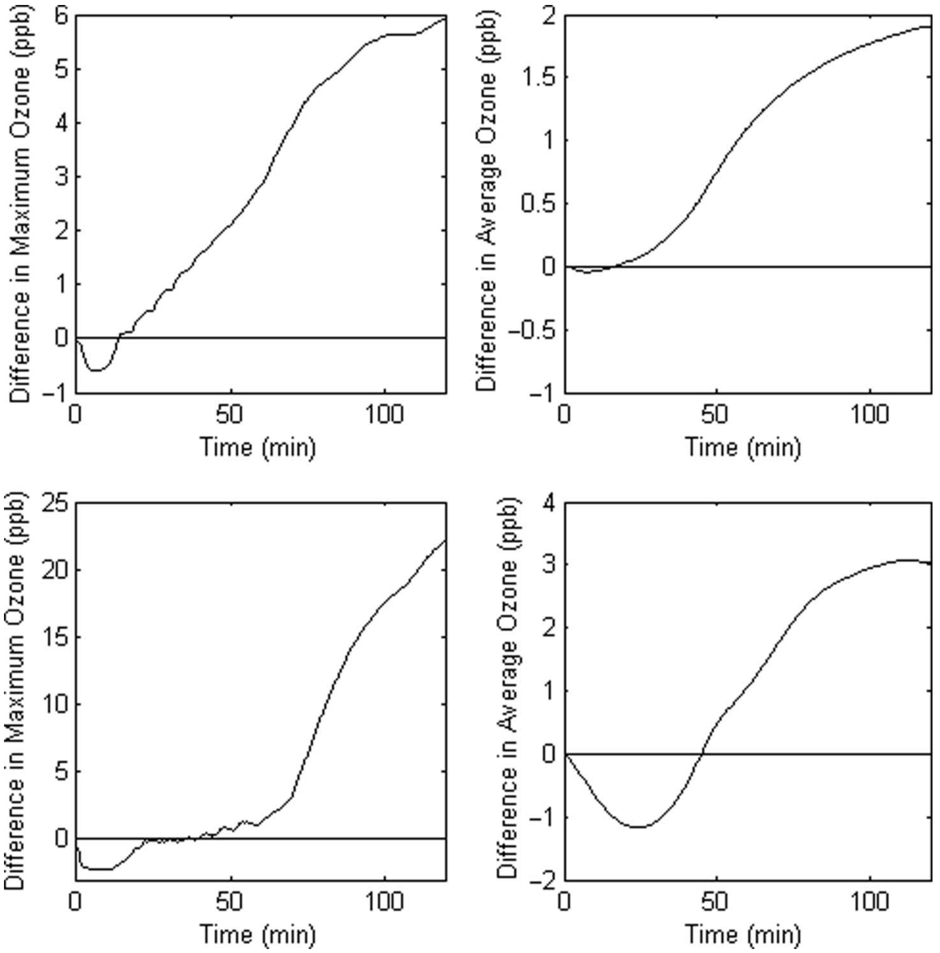

Figure 10. Differences in peak ozone (left) and domain average ozone (right) between 1 km and 200 m resolution runs on a 12 km × 12 km domain for Case 1 (upper) and Case 2 (lower).

Summary and Conclusion

Based on the modeling exercise discussed earlier, we conclude that oil and gas activities can have significant near-source impacts on ambient ozone, through either regular emissions or flares and other emission events associated with process upsets, and perhaps also maintenance, startup, and shutdown of oil and gas facilities. Besides flares, candidate facilities that have the potential to emit large amounts of formaldehyde and/or HRVOCs as well as NO_x in transient events include compressor or drill rig engines, and glycol or amine reboilers used in gas dehydration or sweetening. The enhancement of peak 1-hr ozone by oil and gas activities may exceed 3 ppb approximately 2 km or more downwind, depending on the extent of NO_x titration and inhibition. This ozone enhancement is comparable to the widths of control strategies. Given the possible impact of large single facilities, it is all the more conceivable that aggregations of oil and gas sites may act in concert so that they contribute several parts per billion to 8-hr ozone during actual exceedances. In the past, the U.S. EPA has used a 2-ppb enhancement of ozone above the federal standard as a threshold for regulating significant emission sources, as when Ellis County was brought into the DFW ozone nonattainment area due to the contribution to area episodes attributed to Ellis County cement kilns (Stoeckenius and Yarwood, 2004).

Our findings suggest that improved regulation of the upstream oil and gas industry in nonattainment areas should include reporting of emission events, and more aggressive deployment of control strategies, such as vapor recovery to avoid flaring, and the use of oxidation catalysts on stationary engines. The control of formaldehyde emissions is especially desirable both from an air toxics perspective, and with regard to attainment of the federal ozone standard in surrounding or nearby urban areas.

Lastly, deployment of more contemporary monitoring techniques such as differential optical absorption spectrometry (DOAS) and proton transfer reaction–mass spectrometry (PTR-MS) in place of more conventional methods should be encouraged to better quantify spatially and temporally varying emissions from oil and gas activities, at least in special studies if not in routine regulatory monitoring. Better emission inventories should also be accompanied by the use of air quality models with higher spatial and temporal resolution to more accurately assess the ozone impacts of industry emissions associated with oil and gas exploration and production.

References

Allen, D.T., and V.M. Torres. 2011. *TCEQ 2010 Flare Study, Final Report*. University of Texas at Austin. http://www.tceq.texas.gov/assets/public/implementation/air/rules/Flare/2010flarestudy/2010-flare-study-final-report.pdf (accessed February 15, 2012).

Argo, J. 2011. *Unhealthy Effects of Upstream Oil and Gas Flaring (US SIC 1311 and US SIC 1389)*. Wolfe Island, ON, Canada: IntrAmericas Centre for Environment and Health.

Armendariz, A. 2009. *Emissions from Natural Gas Production in the Barnett Shale Area and Opportunities for Cost-Effective Improvements*. Austin, TX: Environmental Defense Fund.

Bar-Ilan, A., R. Parikh, J. Grant, T. Shah, and A. Pollack. 2008. *Recommendations for Improvements to the CENRAP States' Oil and Gas Emissions Inventories*. Oklahoma City, OK: Central States Regional Air Partnership.

Barnett Shale Energy Education Council (BSEEC). 2010. *Ambient Air Quality Study: Natural Gas Sites, Cities of Fort Worth and Arlington, Texas*. Fort Worth, TX: Titan Engineering Final Report.

Byun, D.W., and J.K.S. Ching. 1999. *Science Algorithms of the EPA Models-3 Community Multiscale Air Quality (CMAQ) Modeling System*. EPA/600/R-99/030. Washington, DC, U.S. Environmental Protection Agency, Office of Research and Development.

Canadian Association of Petroleum Producers. 2004. *A National Inventory of Greenhouse Gas (GHG), Criteria Air Contaminant (CAC) and Hydrogen Sulfide (H2S) Emissions by the Upstream Oil and Gas Industry*. CAPP. http://www.capp.ca/getdoc.aspx?Docid=86224&DT=NTV.

Canadian Association of Petroleum Producers. 2006. *Facility Flare Reduction*. CAPP. http://www.capp.ca/getdoc.aspx?Docid=114231&DT=NTV.

Carter, W.P.L. 2010. *Development of the SAPRC-07 Chemical Mechanism and Updated Ozone Reactivity Scales*. Report to the California Air Resources Board, contracts No. 03-318, 06-408, and 07–730, University of California, Riverside, CA.

Chen, S., X. Ren, J. Mao, Z. Chen, W.H. Brune, B. Lefer, B. Rappenglück, J. Flynn, J. Olson, and J.H. Crawford. 2010. A comparison of chemical mechanisms based on TRAMP-2006 field data. *Atmos. Environ.* 44:4116–4125.

Colella, P., and P.R. Woodward. 1984. The piecewise parabolic method (PPM) for gas-dynamical simulations. *J. Comput. Phys.* 54:174–201.

Eastern Research Group, Inc. 2011. *City of Fort Worth Natural Gas Air Quality Study. Final Report*. Fort Worth, TX, ERG.

Eltgroth, M.W. 2012. *Complex Hazardous Air Release Model (CHARM) Technical Reference Manual*. http://www.charmmodel.com/doc/TechRef_09.pdf (accessed June 14, 2012).

Energy Information Administration. 2006. *Natural Gas Processing: The Crucial Link between Natural Gas Production and its Transportation to Market*. Office of Oil and Gas. http://www.arctigas.gov/sites/default/files/documents/2006-eia-ng-processing.pdf.

Health Effects Institute. 2007. *Mobile-Source Air Toxics: A Critical Review of the Literature on Exposure and Health Effects*. HEI Special Report 16. Boston, MA, HEI.

Hertel, O., R. Berkowicz, and J. Christensen. 1993. Test of two numerical schemes for use in atmospheric transport-chemistry models. *Atmos. Environ.* 27A:2591–2611.

Huang, H.-C., and J.S. Chang. 2001. On the performance of numerical solvers for a chemistry submodel in three-dimensional air quality models, 1. Box model simulations. *J. Geophys. Res.* 106(20):175–20,188.

Kemball-Cook, S., D. Parrish, T. Ryerson, U. Nopmongcol, J. Johnson, E. Tai, and G. Yarwood. 2009. Contributions of regional transport and local sources to ozone exceedances in Houston and Dallas: Comparison of results from a photochemical grid model to aircraft and surface measurements. *J. Geophys. Res.* 114, D00F02. doi:10.1029/2008JD010248

McRae, G.J., W.R. Goodin, and J.H. Seinfeld. 1982. Development of a second generation mathematical model for urban air pollution, I. Model formulation. *Atmos. Environ.* 16:679–696.

Olaguer, E.P. 2011. Adjoint model enhanced plume reconstruction from tomographic remote sensing measurements. *Atmos. Environ.* 45:6980–6986.

Olaguer, E.P. 2012. Near source air quality impacts of large olefin flares. *J. Air Waste Manage. Assoc*. 62:980–990. doi: 10.1080/10962247.2012.693054

Olaguer, E.P., B. Rappenglück, B. Lefer, J. Stutz, J. Dibb, R. Griffin, W.H. Brune, M. Shauck, M. Buhr, H. Jeffries, et al. 2009. Deciphering the role of radical precursors during the second Texas air quality study. *J. Air Waste Manage. Assoc.* 59:1258–1277. doi: 10.3155/1047-3289.59.11.1258

Sander, S.P., R.R. Friedl, D.M. Golden, M. J. Kurylo, G.K. Moortgat, P.H. Wine, A.R. Ravishankara, C.E. Kolb, M.J. Molina, B.J Finlayson-Pitts, et al. 2006. *Chemical Kinetics and Photochemical Data for Use in Atmospheric Studies, Evaluation Number 15*. NASA Jet Propulsion Laboratory 06–2.

Sander, S.P., R.R. Friedl, J.R. Barker, D.M. Golden, M. J. Kurylo, P.H. Wine, J. Abbatt, J.B. Burkholder, C.E. Kolb, G.K. Moortgat, et al. 2010. *Chemical Kinetics and Photochemical Data for Use in Atmospheric Studies, Evaluation Number 16*. NASA Jet Propulsion Laboratory 09–31.

Saunders, S.M., M.E. Jenkin, R.G. Derwent, and M.J. Pilling. 2003. Protocol for the development of the master chemical mechanism, MCM v3 (Part A): Tropospheric degradation of non-aromatic volatile organic compounds. *Atmos. Chem. Phys*. 3:161–180.

Stoeckenius, T., and G. Yarwood. 2004. *Dallas-Ft. Worth Transport Project. Final Report*. Texas Environmental Research Consortium, Houston, TX.

Stutz, J., B. Alicke, and A. Nefte. 2002. Nitrous acid formation in the urban atmosphere: Gradient measurements of NO_2 and HONO over grass in Milan, Italy. *J. Geophys. Res.* 107, 8192–8207. doi:10.1029/2001JD000390

Texas Commission on Environmental Quality. 2007. *Dallas-Fort Worth Attainment and Reasonable Further Progress Demonstrations for the 1997 Eight-Hour Ozone Standard*. Austin, TX, TCEQ. http://www.tceq.texas.gov/assets/public/implementation/airs/sip/dfw/ad_2001/10022SIP_ado_111811.pdf.

Torres, V., D. Allen, and S. Herndon. 2011. TCEQ 2010 Flare Study Report, presented at the Houston-Galveston Area Council, Houston, TX, June 1.

Whitten, G.Z., G. Heo, Y. Kimura, E. McDonald-Buller, D.T. Allen, W.P.L. Carter, and G. Yarwood. 2010. A new condensed toluene mechanism for Carbon Bond: CB05-TU. *Atmos. Environ.* 44:5346–5355.

Wolf Eagle Environmental Engineers and Consultants, LLC. 2009. *Town of DISH, Texas Ambient Air Monitoring Analysis. Final Report*. DISH, TX. http://townofdish.com/objects/DISH_-final_report_revised_pdf.

Yarwood, G., S. Rao, M. Yocke, and G.Z. Whitten. 2005. *Updates to the Carbon Bond Chemical Mechanism: CB05*. Final Report to the U.S. Environmental Protection Agency, RT-04-00675. Research Triangle Park, NC.

About the Author

Eduardo P. Olaguer is a Senior Research Scientist and Director of Air Quality Research at the Houston Advanced Research Center.